行政院國家科學委員會專題研究計畫　成果報告

金屬-氧化鈦複合觸媒微結構之控制與改良(2/2)

計畫類別：個別型計畫
計畫編號：NSC91-2214-E-002-007-
執行期間：91 年 08 月 01 日至 92 年 07 月 31 日
執行單位：國立臺灣大學化學工程學系暨研究所

計畫主持人：吳乃立

計畫參與人員：吳乃立

報告類型：完整報告

處理方式：本計畫可公開查詢

中　華　民　國 92 年 10 月 20 日

行政院國家科學委員會專題研究計畫成果報告
金屬-氧化鈦複合觸媒微結構之控制與改良(2/2)
Microstructural Engineering of metal-titania catalysts
計畫編號：NSC 91-2214-E-002-007
執行期間：91/08/01~92/07/31

主持人：吳乃立　　台灣大學化工系教授

摘要(關鍵詞: 二氧化鈦，氫生成，光觸媒催化，煅燒氣氛，Ar，銅)
本研究主要探討二氧化鈦運用於光觸媒催化由甲醇水溶液中形成氫之相關議題。在此報告中將總結兩項議題之研究結果，包括(1)觸煤煅燒氣氛(2)添加銅顆粒對觸媒活性之影響。二氧化鈦係經由溶膠-凝膠法製成後於 Ar, 合成空氣(air)，氮(N_2), 氫(H_2 3% in N_2) and 真空(vacuum;~5 x 10^{-3} torr) 。對於由甲醇水溶液中形成氫之活性高低次序為 Ar > air> N_2 > vacuum ~ H_2。光譜分析顯示氫與真空導致之低活性源於低表面氫氧基與高晶格缺陷密度。Ar 導致之高活性源於高表面氫氧基及較多之低能隙激發位置(site)。添加表面銅顆粒大幅提昇 TiO_2 活性。光譜分析顯示銅顆粒在反應過程中氧化至具最佳活性之最佳氧化態，而此氧化態無法經由空氣中熱氧化達成。將銅離子溶入氧化鈦晶格中降低活性。

Abstract (Keywords: Titania, hydrogen production, photocatalysis, calcination atmosphere, Ar, Cu)

TiO_2 photocatalysts for hydrogen production from aqueous methanol solution is the main subject of this work, Studies on two issues are reported here, including (1) the effect of calcination atmosphere and (2) the effect of Cu metallization. TiO_2 catalysts were synthesized by a sol-gel process followed by calcination at 400 ^oC in Ar, air, N_2, H_2 (3% in N_2) and vacuum (~5 x 10^{-3} torr), respectively. Toward H_2 production from a water/methanol (vol. ratio= 1.4/1) solution, the catalysts exhibited activities in the order, according to calcination atmosphere, of Ar > air> N_2 > vacuum ~ H_2. The low activity resulting from either vacuum or H_2 calcination was ascribed to a reduced coverage of surface hydroxyl and high bulk defect density, based on the x-ray photoelectron and UV-visible spectroscopic analyses, while the high activity from Ar calcination is to enhanced visible-light excitation. For studying the effect of Cu, Cu particles have been deposited on TiO_2 by incipient-wetness impregnation followed by low-temperature (400 ^oC) calcination/reduction, and the metallization process leads to significant, up to 10 folds, enhancement in photocatalytic activity of TiO_2 for H_2 production from aqueous methanol solution. Spectroscopic studies indicated that the metallic Cu particles were oxidized to have an optimum valence that can not be achieved by thermal oxidation. Dissolution of Cu ion in TiO_2 lattice, in contrast, led to reduction in the activity.

1. Introduction

Photocatalytic production of hydrogen using sunlight as the energy input is a valuable sustainable- energy technology. In this case, solar energy is stored by driving chemical reactions “up-hill” toward chemicals, such as H_2, of higher chemical potentials. Due to its high stability against photocorrosion and its favorite electronic energy band structure, TiO_2 has drawn tremendous attention for such applications. For H_2 production from water, many studies have concluded that direct photo-decomposition of water into H_2 and O_2 has a very low efficiency due to rapid reverse reaction. A much higher hydrogen production rate can be obtained by addition of the “so-called “sacrificial reagents,” such as alcohols and other organics which are oxidized to products that are less reactive toward hydrogen. For H_2 production from a methanol (MeOH) and water solution, depending on reaction condition and whether metal catalyst used, the reaction could proceed either stepwise, involving stable intermediates, such as aldehyde and acid:

$MeOH_{(l)} \leftrightarrow HCHO_{(g)} + H_{2(g)}$ (1)
ΔG^o_1= 64.1 KJ/mole

$HCHO_{(g)} + H_2O_{(l)} \overset{h\nu,\ catal.}{\leftrightarrow} HCO_2H_{(l)} + H_{2\,(g)}$ (2) ΔG^o_2= 47.8 KJ/mole

$HCO_2H_{(l)} \overset{h\nu,\ catal.}{\leftrightarrow} CO_{2(g)} + H_{2(g)}$ (3) ΔG^o_3= -95.8 KJ/mole,
as suggested by Sakata et al., or in one-step on catalyst surface to give the overall reaction:

$MeOH_{(l)} + H_2O_{(l)} \overset{h\nu,\ catal.}{\leftrightarrow} CO_{2(g)} + 3\,H_{2(g)}$ (1) ΔG^o= 16.1 KJ/mole,
as suggested by Chen. H_2 is produced in all of these steps.

The photocatalytic performance of TiO_2 is well known to depend not only on its bulk energy band structure but, to a great extent, on the surface property. The type and density of surface state are affected by, among others, the synthesis process and the use of additional metal particles. The interplay between processing condition and photocatalytic activity remains largely a state-of-art and beyond prediction at this point. Crystalline TiO_2 has typically been calcined and/or crystallized in oxidizing atmospheres, such as air and oxygen. The effect of the so-called "inert" atmospheres, such as N_2, Ar, and vacuum, has mostly been overlooked. Deposition of Pt-group metals, including Ni, Pd and Pt, on TiO_2 photocatalyst has been shown to greatly enhance the photocatalytic production of H_2 from either pure water or water/sacrificial reagent solutions. Sakata et al. [A4] attributed the enhancement to the catalytic effects of the metal particles on H_2 evolution. Millard and Bowker [B2], on the other hand, suggested that the presence of Pd provides a reaction pathway which involves chemisorption and dehydrogenation of MeOH on Pd to produce chemisorbed CO and subsequent oxidation of the chemisorbed CO to CO_2.
Cu-containing TiO_2 catalyst is well known for their photocatalytic activity toward CO_2 reduction [C1-C4] but much less known for its performance in H_2 production from water

In this report, we summarize our research results on two issues: (1) effect of calcination atmospheres, including Ar, air, N_2, H_2 and vacuum (~5 x 10^{-3} torr); and (2) the effect of Cu-metallization.

2. Experimental

TiO_2 powder was synthesized by a conventional sol-gel process. $TiCl_4$ was first dissolved in an ethanol/water (volume ratio= 4:1) solution, and ammonia was then introduced into the solution to induce condensation until pH reached 7.5. The resulted gelatinous precipitate was filtered and washed, primarily to remove Cl^-, and then dried at 65 ^oC in air. Calcination of xerogel was carried out in Ar, synthetic air (N_2/O_2 mol ratio= 79:21), nitrogen, hydrogen (3mol % in N_2), and vacuum (~$5x10^{-3}$ torr), respectively. Calcination procedure started with purging the reactor with the selected gas (in the case of vacuum treatment, the reactor was evacuated to ~$5x10^{-3}$ torr) for 1 hr, heated the powder at a rate of 100 ^oC/hr to 400 ^oC, and held the powder at 400 ^oC for 1 hr before finally the powder being furnace-cooled.

Cu was loaded by an incipient-wetness method, in which an aqueous solution containing $CuCl_2 \cdot 2H_2O$ was added to the oxide powder in an amount that was just sufficient to wet completely the powder. The resulted powder was then dried and calcined in synthetic air (N_2/O_2 mol ratio= 79:21) to make the catalyst. The powders were calcined by following the standard calcination procedure. The catalyst powders were stored as calcined, and they were further reduced at 400 ^oC by H_2 (3 mol % in N_2) for 3 hrs prior to characterization works, including the spectroscopic and kinetic analyses.

Kinetic experiments were carried out by using a vertical tubular batch reactor made of quartz. During a typical run, the entire reactor was enclosed inside a UV-light house (Rayonet photochemical reactor, RPR-100), and the reactor was half-filled with a water/MeOH (H_2O/MeOH vol. ratio= 1.4:1) solution, in which the oxide particles, in an amount of 1.25 g/liter, were constantly dispersed by a magnetic stirrer. The light house was equipped with 16 UV-light (maximum intensity at 300 nm) tubes, each having a power of 12 W. The unfilled space above the solution was evacuated at the beginning of reaction, and H_2 concentration was determined intermittently by extracting a small volume of the gas-phase product for gas chromatography (GC) analysis. The accumulative H_2 production data were then calculated from the concentration data, assuming ideal-gas behavior.

3. Results and Discussion

3.1 Effect of calcination atmosphere

As shown in Fig. 1, upon UV irradiation, H_2 was produced with steadily increasing concentration with time until it saturated at a steady level. In a batch reactor, such as the one currently employed, a steady state represents equilibrium. The H_2 and vacuum calcined catalyst was found to exhibit the worst performance, while the air- and N_2-calcined catalysts showed another level of performance. The Ar-calcined catalyst, on the other hand, gave overall the best performance in terms of both the maximum rate and equilibrium production level. It is also superior to the commercial P25 catalyst.

Figure 2 shows the diffuse reflectance UV-VIS spectra. The absorption edge energy is determined by Tauc plot $[(\alpha h\nu)^2$ vs $h\nu$, where α is the absorbance] for semiconductors with the direction transition. Except for the vacuum-calcined catalyst, which appears black, all the catalysts show a sharp UV absorption near 3.25 eV, consistent with the theoretical band gap energy of anatase TiO_2. Significant

differences, however, exist in absorption within the visible-light range next to the absorption edge. The Ar, air and N_2 samples showed visible-light absorption correlated consistently with their activities, showing increasing activity with increasing absorption. On the other hand, the vacuum and H_2 samples both showed stronger visible-light absorptions but yet lower activities than the rest catalysts.

XPS studies indicated mainly two types of surface properties. The Ar- and air-calcined catalysts showed higher Ti and O binding energies than the other catalysts (Fig. 3). The binding energies of Ti (459.7 ± 0.2 eV for Ti $2P_{3/2}$) for the Ar and air samples are typical of Ti^{+4}. A red shift by ~2.2 eV observed on the other samples indicates the presence of Ti^{+3} therein. For the O (1s) XPS peak, the differences indicate the air- and Ar calcined catalysts have a higher surface coverage of hydroxyl group than the other catalysts.

For a semiconductor-photocatalyzed reaction, the reaction rate is basically determined by how fast the charged particles, including the valence-band hole and conduction-band electron, are generated and the how efficiently they are transferred to the reactants at surface before they recombine. Two opposite effects related to photocatalysis could result from defects which provide energy states in the band gap. On the one hand, they could enable excitation with photon energy lower than the band gap energy and hence facilitates excitation to form the charged particles. On the other, they would also act as scattering centers to slow down the transport of charged particles to surface where reaction takes place. As a result, an optimum density, as well as an optimum property, of the structure defect is expected for good photocatalysis performance. This may explain the observation that there appears to be an optimum visible-light absorption level for maximum reaction rate (Fig. 2). For the Ar, air and N_2 samples, the photocatalytic activity was found to increase with increasing the absorption. This may suggest that the defect density is low enough that the excitation effect is predominant. In contrast, the excitation effect might be severely offset by the scattering effect in the cases of the vacuum and H_2 samples, which showed very strong visible-light absorptions but yet poor performance.

Another strong clue to the cause of the reactivity variation is provided by the XPS data, which showed difference in the surface hydroxyl coverage. It has been shown that >TiOH, the so-called surface “titanol” group, is an important trapping center for the valence-band hole and hence the principal oxidizing site in the photoactivated TiO_2. Reduced hydroxyl coverage would thus impair the activity of the catalyst. This might also contribute, in part, to the poor performance exhibited by the vacuum- and H_2-calcined samples. An intermediate level of visible-light absorption level combined with high surface hydroxyl coverage render the Ar –calcined catalyst the highest photocatalytic activity.

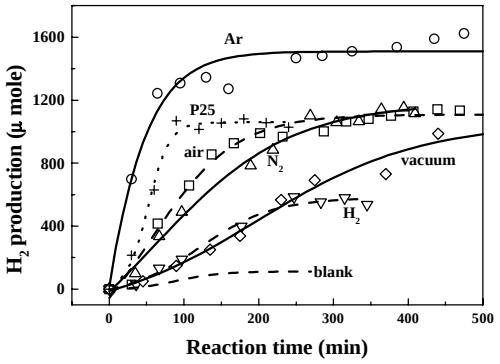

Figure 1. H_2 generation curves.

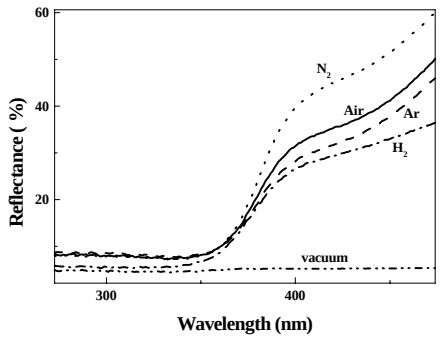

Figure 2. Diffuse reflectance spectra of TiO_2 .

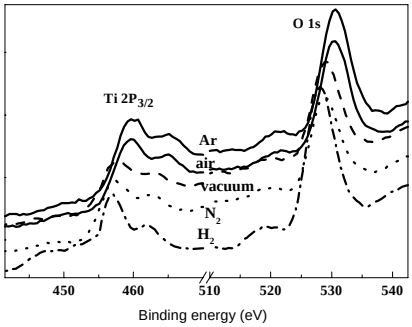

Figure 3. XPS spectra of TiO_2 catalysts.

3.2 The effect of Cu metallization

The blank TiO_2 catalyst (Cu loading = 0 wt%) appeared yellowish. With increasing Cu deposition up to 1.9 wt% of Cu, the catalysts turned increasing reddish, but XRD did not detect reflection of Cu. The grain size of TiO_2, being insensitive to the Cu content, was slightly increased to ~ 10.0 nm, presumably caused by additional reduction heat treatment. The BET surface area is 110 m/g.

UV-VIS spectroscopic analysis (Fig. 4) of the blank TiO_2 showed a major UV-absorption near 350 nm wavelength and a minor one near 450 nm. The latter is consistent with its yellowish appearance. Determined by Tauc plot the major absorption edge energy is close to the theoretical value (3.20 eV) of anatase TiO_2. Deposition of Cu caused a reduction in major edge energy to 3.09 eV and a dramatic increase in visible-light absorption. The absorption extends up to 700 nm in wavelength, which is also consistent with their reddish appearance, and the absorbance increased with increasing Cu content. XPS of the Cu-deposited catalysts detected only Cu, Ti, O, and C. The detected Cu (2p3/2) binding energy (930.5 eV; Fig. 5) is assigned to be metallic Cu. Quantitative analysis considering only the first three elements gave almost the same (±2% variation) Cu content as the loaded value, suggesting that Cu was indeed largely deposited on TiO_2 surface, rather than embedded within TiO_2 matrix.

Figure 6 summarizes the H_2-generation curves for catalysts of different Cu loading. For comparison, data from a commercial TiO_2 (P25, Degussa) was also shown (Fig. 6). The fitted $dP/dt\,|_{max}$, P_{eq} data are summarized in Fig. 7. They were found to follow the same trend against Cu loading, showing a maximum at 1.2 wt% of Cu. The maximum production rate at the optimum Cu content is 10 times that of the blank TiO_2 and 4.5 times that of P25.

The occurrence of an optimum metal loading is indicative of interfacial active sites at and/or near the peripheries of the Cu particles. The total peripheral length increases with increasing Cu particle number and size until reactive domains begin to overlap. Further increase in Cu loading would only lead to reduction of the peripheral length, and hence the reactivity. It was also noticed that the catalysts, which appeared reddish at the beginning of the reaction, turned greenish after reaction, suggesting oxidation of Cu. This was confirmed by XPS (Fig. 5), which showed an increase by 1 eV in Cu (2p3/2) binding energy to ~931.5 eV. The result indicated that it is an oxidized Cu species that is active. Two types of oxidized Cu-TiO_2 catalysts (1.2 wt% of Cu) were thus prepared for comparison. The first one was oxidized, after the thermal reduction procedure, by prolonged (5 days) exposure in air at room temperature, while the second one was heated in air at 400 ^oC for 1 hr. The former appeared dark brownish, while the latter dark green. Both catalysts did show significant photocatalytic activities (Fig. 8) but were inferior to the freshly reduced catalyst. XPS showed that Cu in these two catalysts exhibited higher binding energies, hence higher valences than that oxidized in situ during the reaction. In particular, the Cu (2p3/2) binding energy (932.3 eV) for the catalyst oxidized at room temperature (Fig. 5) is consistent with Cu^{+1} in Cu_2O, and therefore the Cu in the reaction-oxidized catalyst has an average valence between 0 and +1.

Finally, it is pointed out that kinetic study on catalyst prepared by mixing the Cu and Ti sources, namely $CuCl_2$ and $TiCl_4$, at the very beginning of the synthesis process has also indicated that Cu-doping within the TiO_2 lattice has a negative effect on the overall catalytic activity.

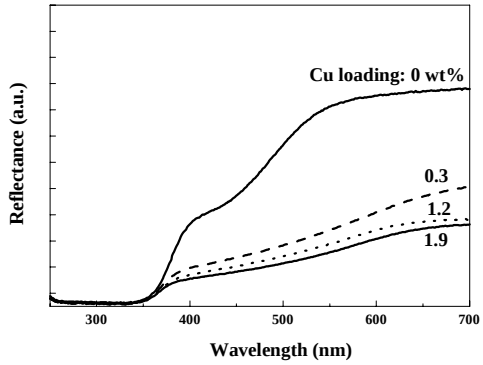

Figur4. Diffuse reflectance spectra of Cu-TiO_2 catalysts.

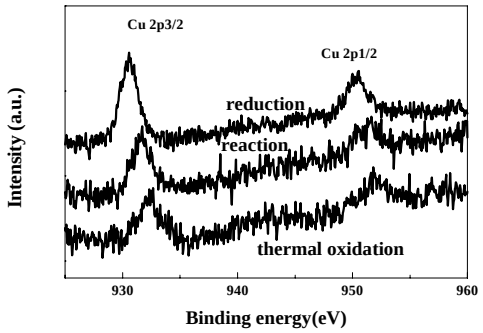

Figure 5. Cu XPS spectra of the Cu-TiO_2 catalysts

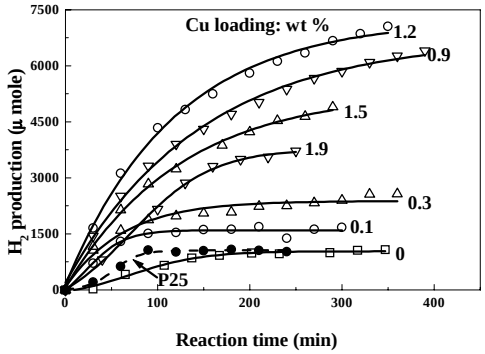

Figure 6. H_2 generation curves for the Cu-TiO_2.

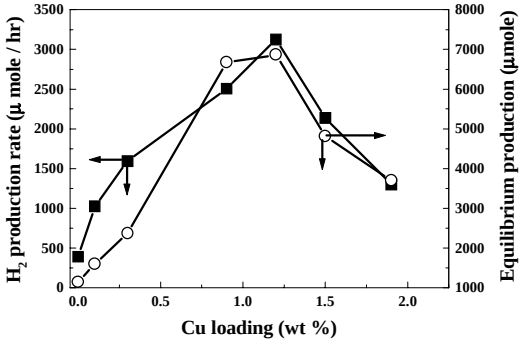

Figure 7. Effect of Cu loading on H_2 production rate and equilibrium production.

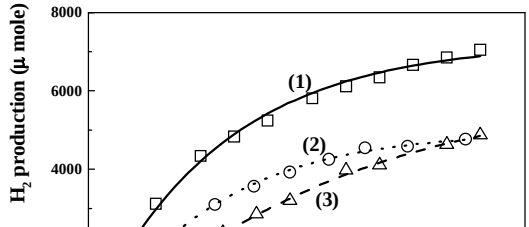

Figure 8. Effect of Cu oxidation on H_2 production. Key: (1) oxidation in situ by reaction; (2) thermal oxidation at 400 ^{o}C in air for 1 hr; (3) thermal oxidation in air at room temperature for 120 hr. Cu loading is the same (1.2 wt %).

5. References

1. .T. Kawai and T. Sakata, J.C.S. Chem. Comm. (1980) 694.
2. T. Sakata, T. Kawai, and K. Hashimoto, Chem. Phys. Lett. 88, 50 (1982).
B1. J. Chen, D. F. Ollis, W. H. Rulkens, and H. Bruning, Wat Res. 33, 669 (1999).
B2. L.Millard and M. Bowker, J. Photochem. Photobiol. A 148, 91 (2002).